Corrosion Science, Vol. 19, pp. 907 to 920
Pergamon Press Ltd. 1979. Printed in Great Britain.

ELECTROCHEMICAL AND CORROSION BEHAVIOUR OF WORK-HARDENED COMMERCIAL AUSTENITIC STAINLESS STEELS IN ACID SOLUTIONS*

B. Mazza, P. Pedeferri, D. Sinigaglia, A. Cigada, G. Fumagalli and G. Re

Istituto di Chimica-Fisica, Elettrochimica e Metallurgia del Politecnico di Milano, Centro di Studio del CNR sui Processi Elettrodici, Piazza Leonardo da Vinci 32, 20133 Milano, Italy

Abstract—This paper describes the results of a study concerning the electrochemical and corrosion behaviour of AISI Types 304L and 316L stainless steels, cold worked under various conditions, in 1M H_2SO_4 and in 0.1M HCl de-aerated solutions. Anisotropic behaviour of specimen surfaces with different orientations to the direction of deformation has been observed. Stress corrosion cracking of the deformed steels can occur at room temperature in the 0.1M HCl solution both in the active and transition regions of the polarization curves.

INTRODUCTION

A systematic study of the influence of cold plastic deformation on the electrochemical and corrosion behaviour of commercial austenitic stainless steels in different aggressive media has been carried out in this laboratory from 1970 onwards,[1-9] and is now coming to an end. In this paper a general view is given of the results concerning the AISI Types 304L and 316L stainless steels submitted to cold plastic deformation under various conditions and then immersed in 1M H_2SO_4 and in 0.1M HCl de-aerated solutions at 25°C.

EXPERIMENTAL METHOD

Materials were first annealed at 1050°C for 1h and water quenched, then submitted to cold plastic deformation by either tension, drawing, or rolling, at room temperature (25°C) or at liquid nitrogen temperature (−196°C). The chemical composition of the stainless steels under study is given in Table 1.

Specimens were cut so as to obtain different orientations of the surface exposed to the aggressive medium, with respect to the direction of deformation. Longitudinal (L) and transverse (T) surfaces in the case of both tension and drawing, and longitudinal (L), long-transverse (T_L) and short-transverse (T_S) surfaces in the case of rolling were considered.

A detailed description of the procedure for specimen surface preparation, of the polarization cell and electrode assembly is given elsewhere.[4-7] Saturated mercurous sulphate reference electrodes (SSE) were used.†

Conventional polarization measurements were conducted potentiodynamically. Moreover the cyclic polarization (or electrochemical hysteresis) technique[10-16] was applied for investigating pitting resistance in the HCl solution. Lastly, potentiostatic measurements were performed in the HCl solution in order to study the stress corrosion cracking of the deformed steels.

After the electrochemical tests, the specimens were removed from the assembly and examined under a metallographic microscope.

EXPERIMENTAL RESULTS

Some results of the conventional electrochemical tests are given in Figs 1–4.

*Manuscript received 25 January 1979.

†The potential of the SSE referred to a standard hydrogen electrode is +642 mV at 25°C.

TABLE 1. CHEMICAL COMPOSITION OF THE COMMERCIAL AUSTENITIC STAINLESS STEELS UNDER STUDY

Steel type	Composition (wt%)										Subsequent cold working
	C	Si	Mn	P	S	Cr	Ni	Mo	Cu	N	
AISI 304L	0.025	0.45	1.39	0.023	0.021	18.60	8.75	0.50	0.24	0.036	Tension
	0.032	0.54	1.64	0.009	0.009	18.60	8.70	0.48	0.20	0.038	Drawing
	0.020	0.41	1.40	0.032	0.013	18.10	10.30	0.32	0.24	0.039	Rolling
AISI 316L	0.022	0.43	1.51	0.033	0.023	16.80	10.65	2.90	0.07	0.033	Tension
	0.023	0.40	1.45	0.034	0.021	16.60	10.90	3.00	0.08	0.037	Drawing
	0.026	0.41	1.24	0.008	0.011	16.10	10.90	2.20	0.07	0.034	Rolling

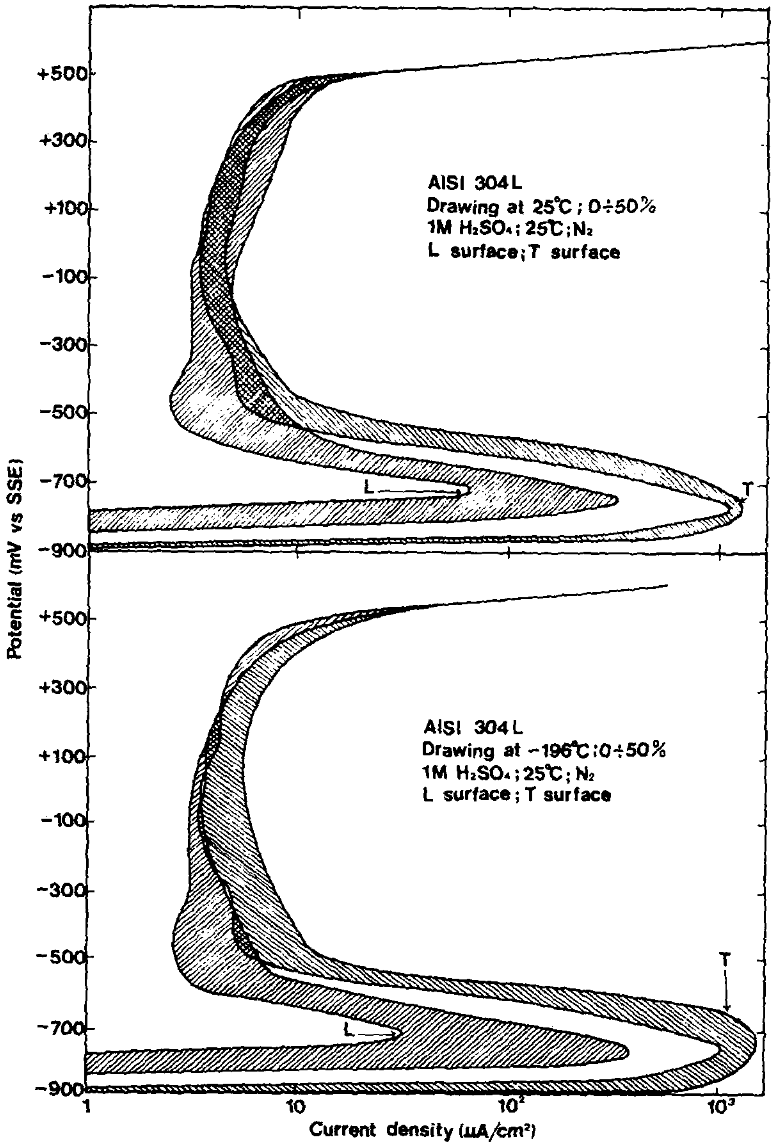

Fig. 1. Potentiodynamic anodic polarization curves (sweep rate 30 mV min^{-1}) for AISI Type 304L stainless steel in de-aerated 1M H_2SO_4 solution at 25°C, indicating the effect of the degree of deformation (0–50% within the shaded areas) and of the orientation of the specimen surface to the direction of deformation (L = longitudinal and T = transverse surfaces). Deformation by drawing at both room and liquid nitrogen temperatures. Potential values refer to a saturated mercurous sulphate electrode (SSE).

The main data obtained from the potentiodynamic anodic polarization curves, i.e. critical current density for passivation (i_{cr}), primary passivation potential (E_{pp}) and

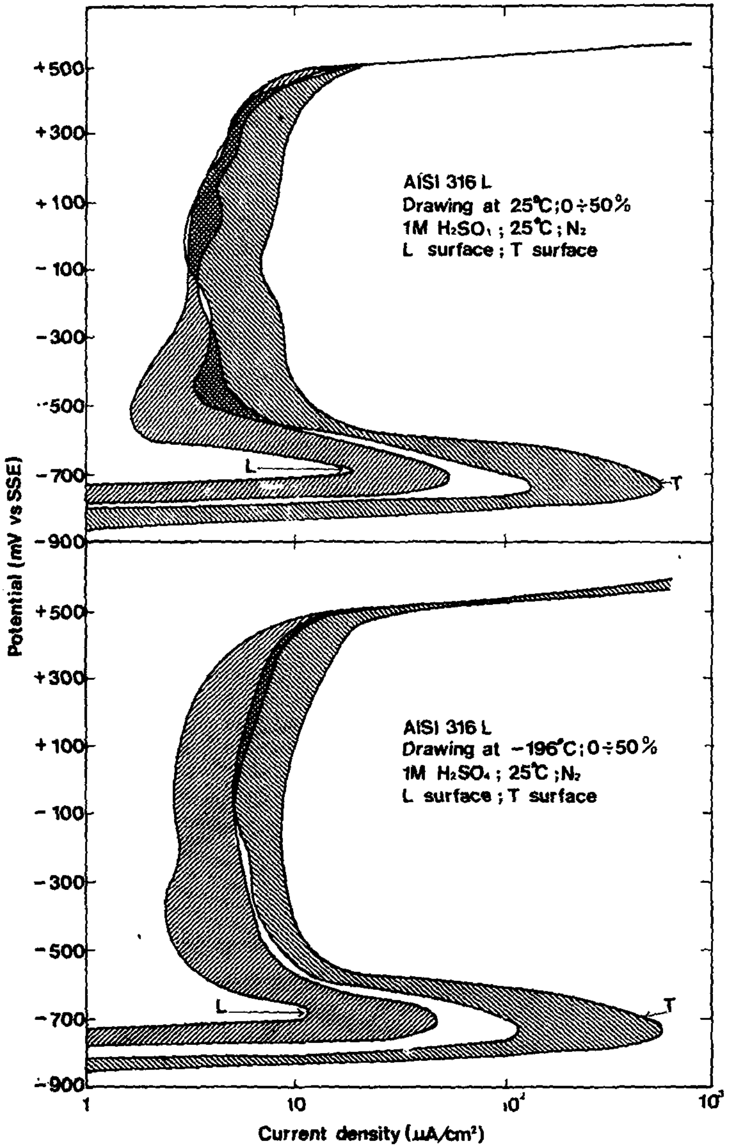

FIG 2. Potentiodynamic anodic polarization curves (sweep rate 30 mV min^{-1}) for AISI Type 316L stainless steel in de-aerated 1M H_2SO_4 solution at 25°C, indicating the effect of the degree of deformation (0–50 % within the shaded areas) and of the orientation of the specimen surface to the direction of deformation (L = longitudinal and T = transverse surfaces). Deformation by drawing at both room and liquid nitrogen temperatures.

critical pitting potential (E_c)*, were plotted vs degree of deformation for the different

*In the case of work-hardened materials exposed to the HCl solution, pitting is often superimposed upon general corrosion, i.e. the material surface is pseudo-passive[17] (see Figs 3 and 4). In this case the term 'critical pitting potential' is used for that potential at which the transition from pseudo-passivity to a process of localized corrosion takes place, i.e. that potential at which the current density begins increasing again after the primary anodic loop of the polarization curve.

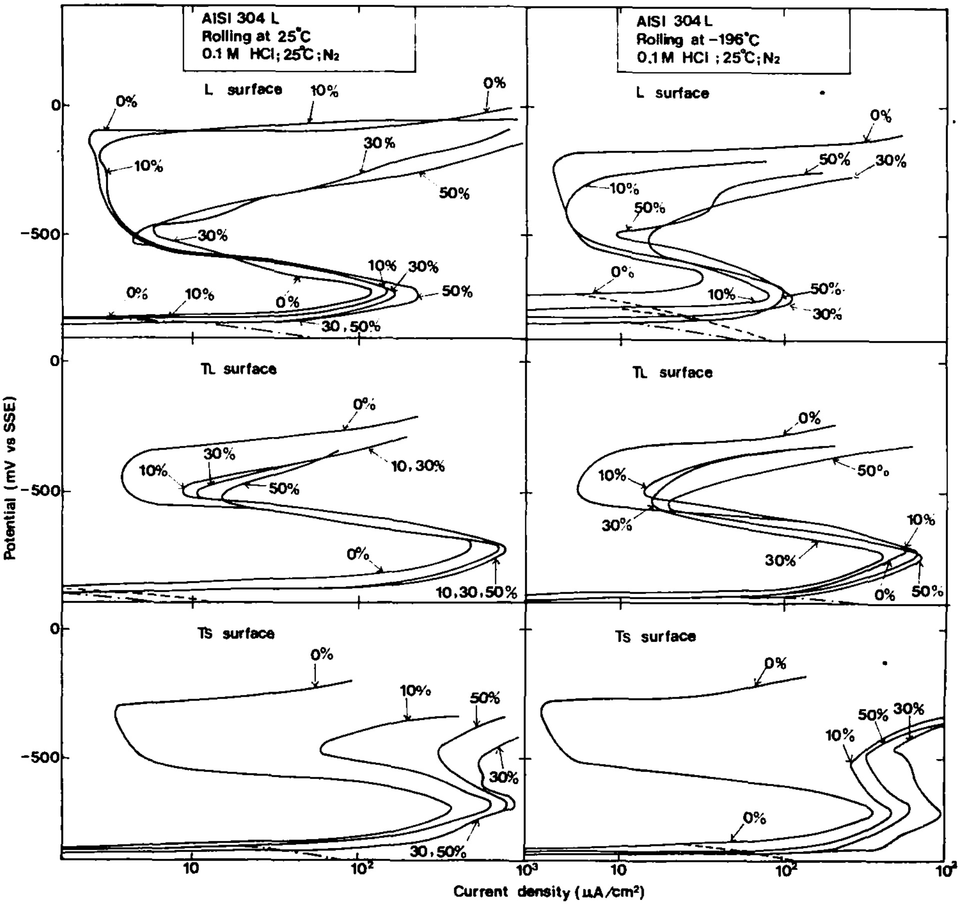

FIG. 3. Potentiodynamic anodic polarization curves (sweep rate 30 mV min^{-1}) for AISI Type 304L stainless steel in de-aerated 0.1M HCl solution at 25°C, indicating the effect of the degree of deformation (0–50%) and of the orientation of the specimen surface to the direction of deformation (L = longitudinal, T_L = long-transverse, and T_S = short-transverse surfaces). Deformation by rolling at both room and liquid nitrogen temperatures.

types and temperatures of cold working, and for the different orientations of the specimen surface to the direction of deformation (Figs 5–7).

Both in 1M H_2SO_4 (Figs 1 and 2) and in 0.1M HCl (Figs 3–7) solutions, the critical current density for passivation and the primary passivation potential are not affected significantly by the cold work characteristics, i.e. type, temperature and degree. The anisotropic behaviour of specimen surfaces with different orientations to the direction of deformation should be emphasized: the surfaces parallel to the direction of deformation generally exhibit a lower critical current density for passivation than the transverse ones.*

---

*This anisotropy is shown even by an undeformed material.

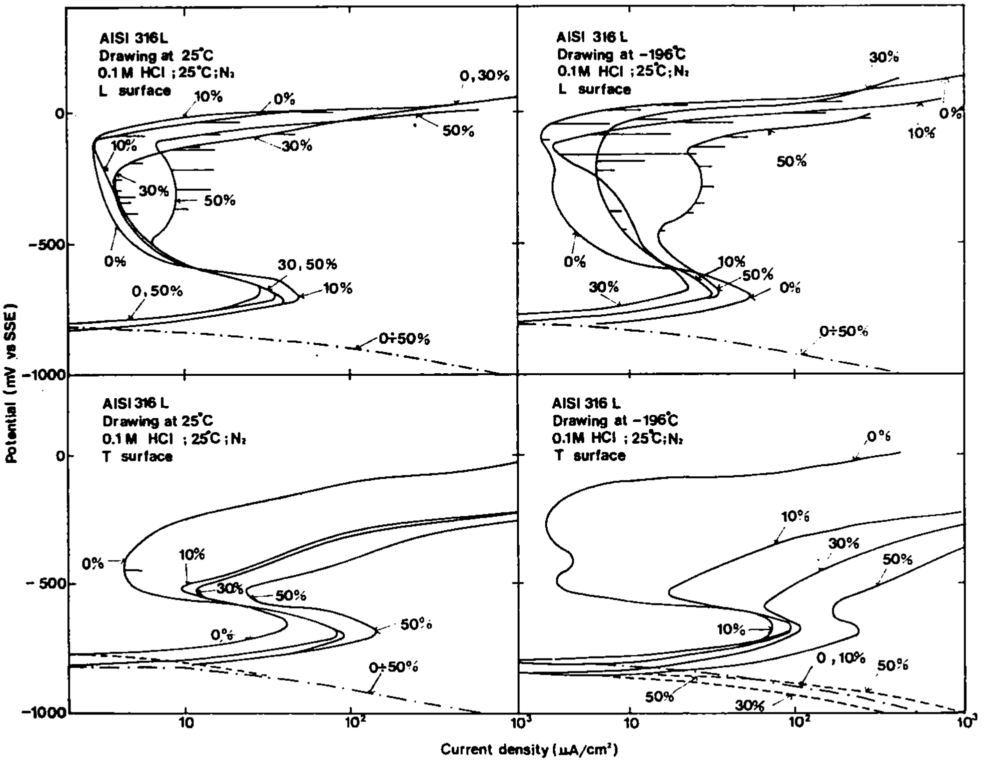

FIG. 4. Potentiodynamic anodic polarization curves (sweep rate 30 mV min^{-1}) for AISI Type 316L stainless steel in de-aerated 0.1M HCl solution at 25°C, indicating the effect of the degree of deformation (0–50%) and of the orientation of the specimen surface to the direction of deformation (L = longitudinal and T = transverse surfaces). Deformation by drawing at both room and liquid nitrogen temperatures. The horizontal lines indicate repassivation of small pits.

On exceeding the primary passivation potential, in the case of the 1M H_2SO_4 solution, the orientation of the specimen surface, as well as the degree, type and temperature of the cold work do not exert any significant influence on the characteristic parameters (i.e., passivity current density and transpassivity potential) of the passivity region of the polarization curves (Figs 1 and 2).

In the 0.1M HCl solution, the critical pitting potential generally decreases with increase in the degree of deformation and moreover, for every given value of the latter, it decreases when passing from the longitudinal to the transverse surfaces* (Figs 3–7). In accordance with these observations, the passivity region of both the conventional (Figs 3 and 4) and the cyclic (Figs 8 and 9) polarization curves, and the hysteresis loops of the cyclic polarization curves (Figs 8 and 9) become smaller and smaller until they finally disappear, i.e. the surface film becomes less and less

---

*This anisotropic behaviour is shown also by steels not deformed by cold work.

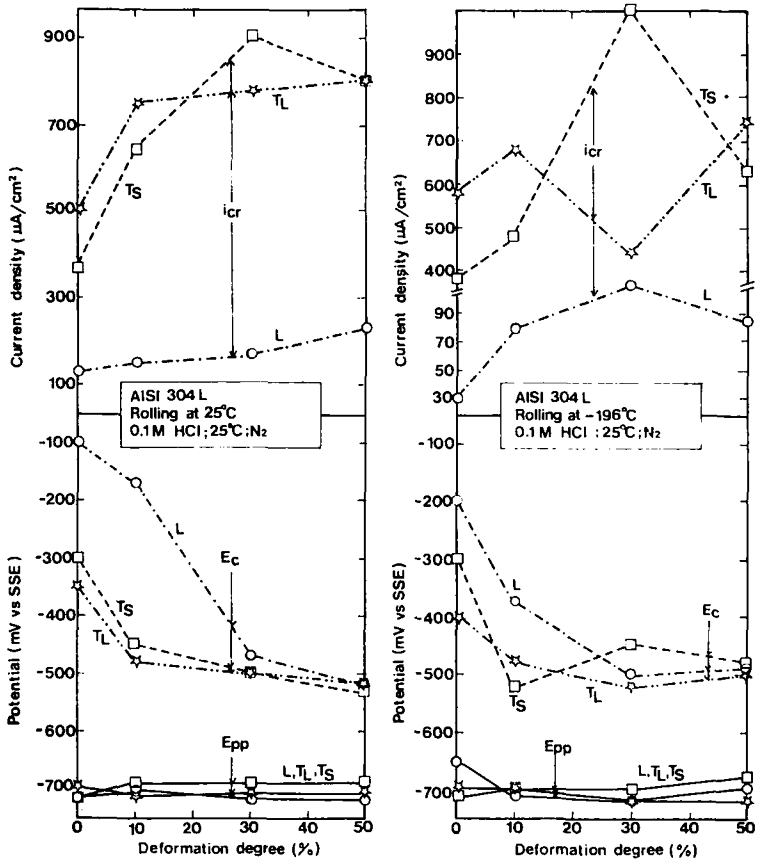

FIG. 5. Critical anodic current density for passivation (i_{cr}), primary passivation potential (E_{pp}) and critical pitting potential (E_c, determined by the conventional scanning method, sweep rate 30 mV min^{-1}) vs degree of deformation for different orientations of the specimen surface to the direction of deformation (L = longitudinal, T_L = long-transverse, and T_S = short-transverse surfaces), in the case of AISI Type 304L stainless steel in de-aerated 0.1M HCl solution at 25°C. Deformation by rolling at both room and liquid nitrogen temperatures.

stable and less and less protective (pseudo-passivity condition*[17]); at the same time, the morphological aspects of the attack tend to change from those typical of pitting to those of an uneven general corrosion type.

A comparison between the steels under study regarding their pitting resistance in the 0.1M HCl solution, shows that the 316L with exposed transverse surfaces becomes similar in behaviour to the 304L steel at the higher degrees of deformation (see Figs 5–7).

*For exposed transverse surfaces, at the higher degrees of deformation, the reduction in the current density which follows the active dissolution region of the polarization curves cannot be taken as a true passivation because of the high current densities involved.

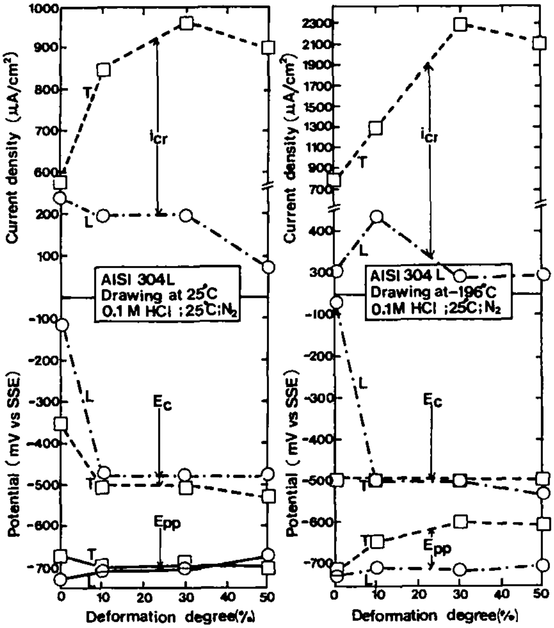

FIG. 6. Critical anodic current density for passivation (i_{cr}), primary passivation potential (E_{pp}) and critical pitting potential (E_c, determined by the conventional scanning method, sweep rate 30 mV min^{-1}) vs degree of deformation for different orientations of the specimen surface to the direction of deformation (L = longitudinal and T = transverse surfaces), in the case of AISI Type 304L stainless steel in de-aerated 0.1M HCl solution at 25°C. Deformation by drawing at both room and liquid nitrogen temperatures.

Stress corrosion cracking of the deformed steels can develop under potentiostatic conditions at room temperature in the 0.1M HCl solution both in the active and transition regions of the polarization curves (Figs 10–12), in accordance with the results of other authors concerning conditions of applied constant stress or strain.[18–20] This form of attack has been observed only in the case of deformation by drawing at the liquid nitrogen temperature, for high degrees of deformation on transverse surfaces. An uneven general corrosion is always superimposed.

A comprehensive discussion of the main aspects of the general and localized corrosion behaviour of work-hardened commercial austenitic stainless steels in relation to characteristic structural effects of the cold plastic deformation[8] (dislocations, deformation bands, martensite transformation, and role of the nonmetallic inclusions), is given elsewhere [7,9] and in papers under preparation.

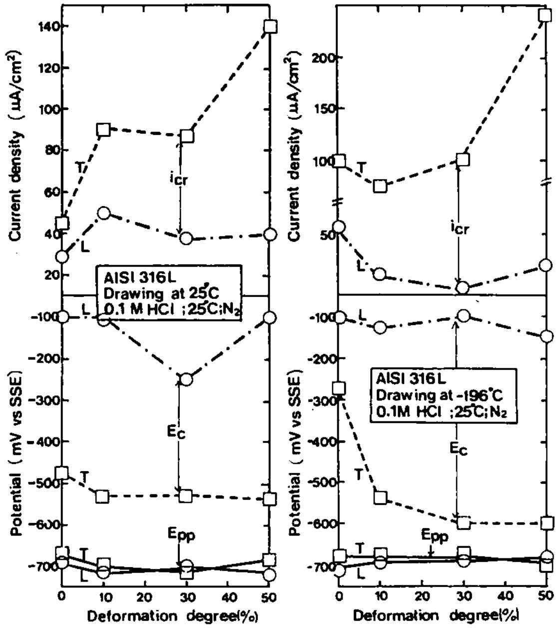

FIG. 7. Critical anodic current density for passivation (i_{cr}), primary passivation potential (E_{pp}) and critical pitting potential (E_c, determined by the conventional scanning method, sweep rate 30 mV min^{-1}) vs degree of deformation for different orientations of the specimen surface to the direction of deformation (L = longitudinal and T = transverse surfaces), in the case of AISI Type 316L stainless steel in de-aerated 0.1M HCl solution at 25°C. Deformation by drawing at both room and liquid nitrogen temperatures.

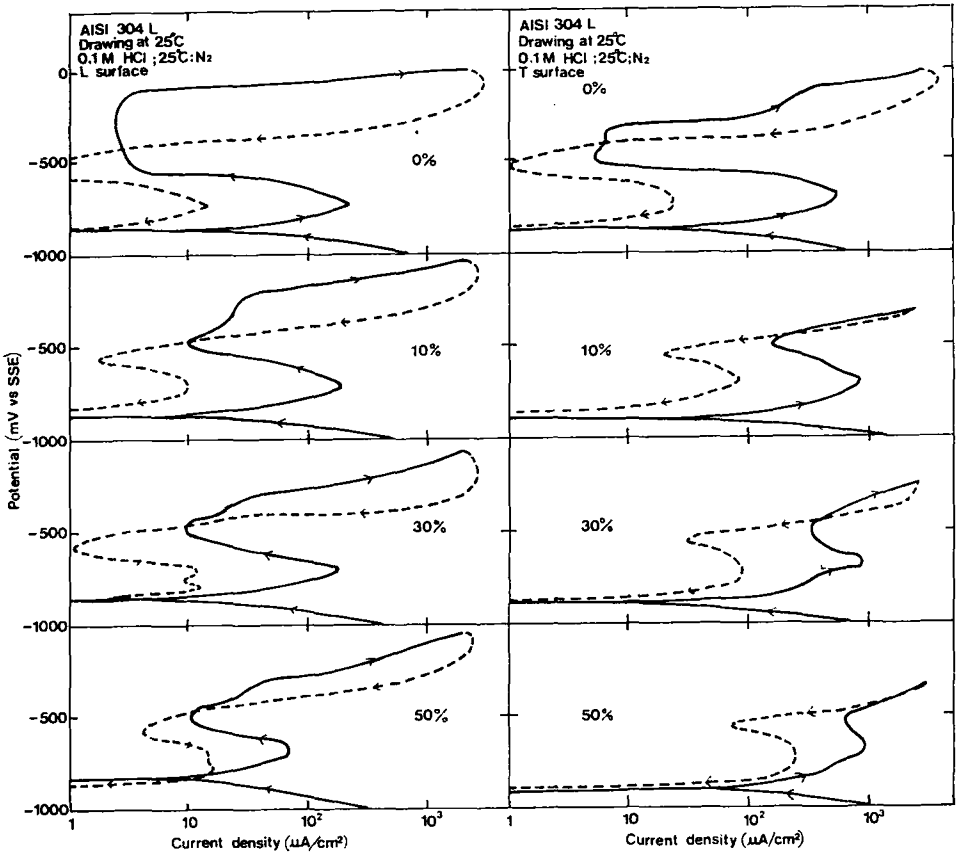

FIG. 8. Cyclic potentiodynamic anodic polarization curves (sweep rate 30 mV min^{-1}) for AISI Type 304L stainless steel in de-aerated 0.1M HCl solution at 25°C, indicating the effect of the degree of deformation (0–50 %) and of the orientation of the specimen surface to the direction of deformation (L = longitudinal and T = transverse surfaces). Deformation by drawing at room temperature.

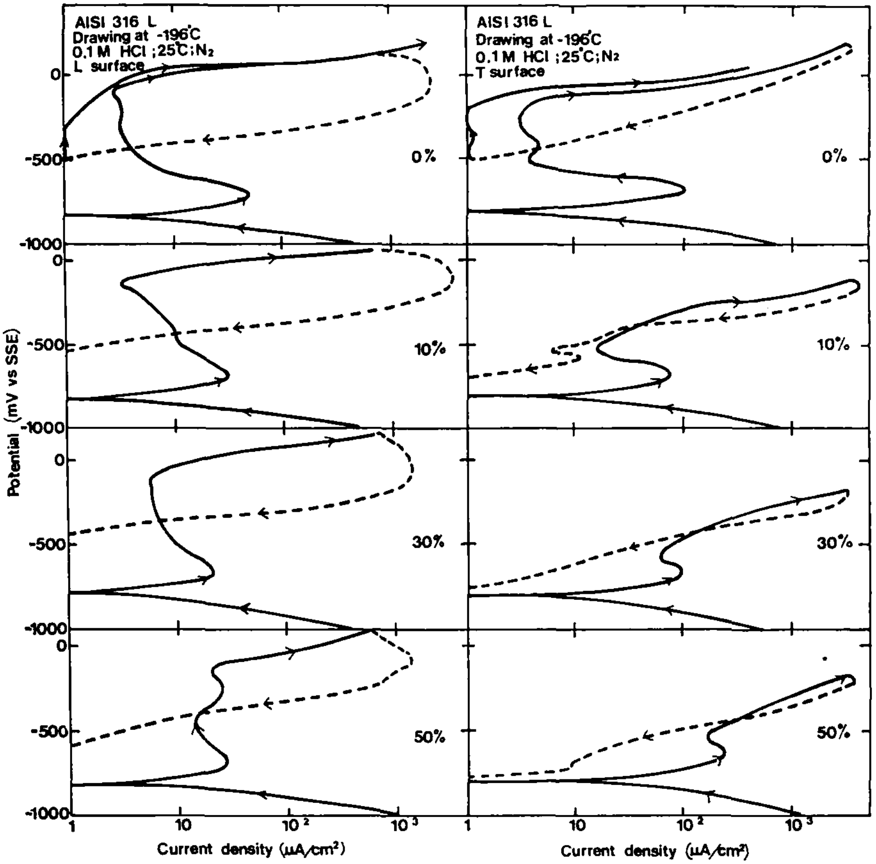

FIG. 9. Cyclic potentiodynamic anodic polarization curves (sweep rate 30 mV min^{-1}) for AISI Type 316L stainless steel in de-aerated 0.1M HCl solution at 25°C, indicating the effect of the degree of deformation (0–50%) and of the orientation of the specimen surface to the direction of deformation (*L* = longitudinal and *T* = transverse surfaces). Deformation by drawing at liquid nitrogen temperature.

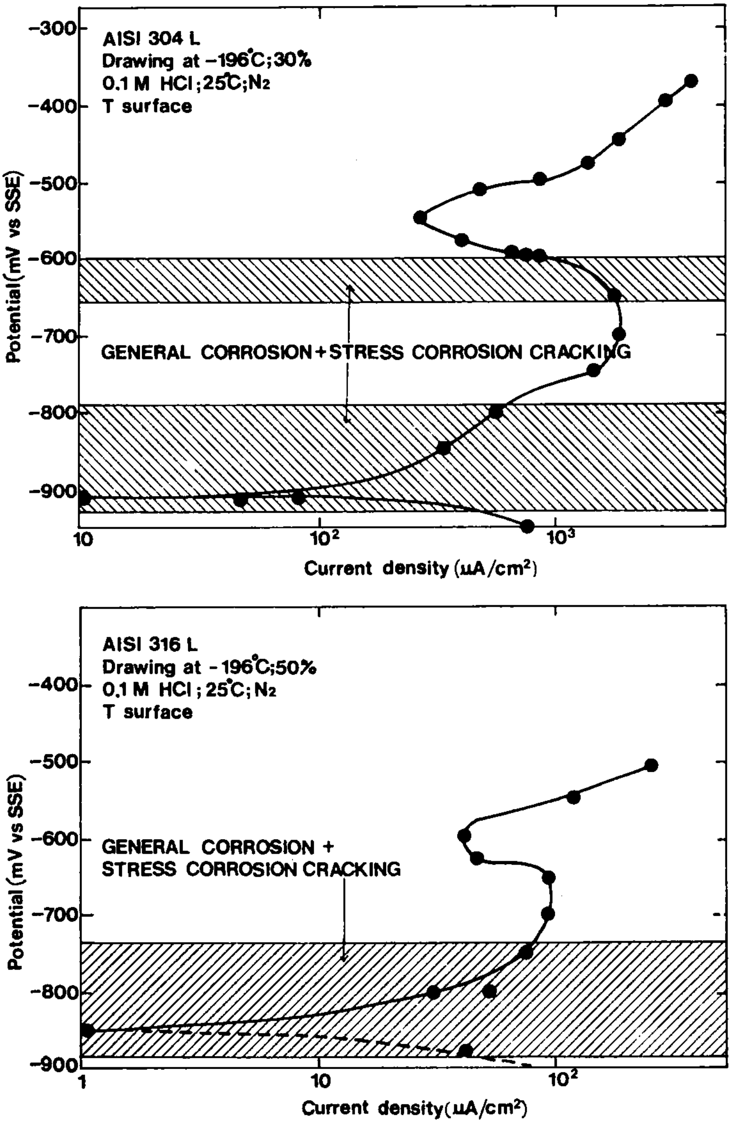

Fig. 10. Potentiostatic measurements on deformed AISI Types 304L and 316L stainless steels in de-aerated 0.1M HCl solution at 25°C, showing the types of corrosion observed. Deformation by drawing at liquid nitrogen temperature; deformation degree 30% for the 304L and 50% for the 316L steel; transverse surfaces exposed. A new specimen has been utilized for each measurement. Exposure times 10–60 min.

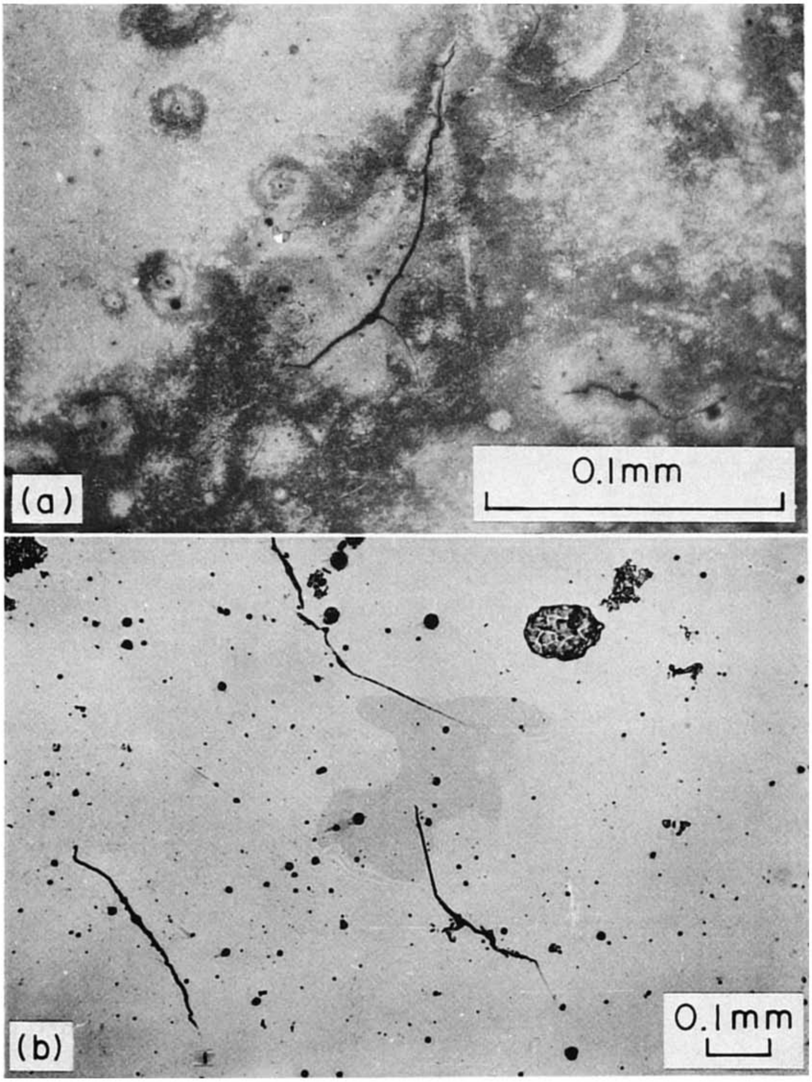

FIG. 11. Stress corrosion cracking of deformed AISI Type 304L stainless steel in de-aerated 0.1M HCl solution at 25°C, 10 min exposure at −800 mV vs SSE (active range). Deformation by drawing at liquid nitrogen temperature; deformation degree 30%; transverse surface exposed.

(a) After washing with distilled water, (b) after polishing with 1/4 μm diamond paste.

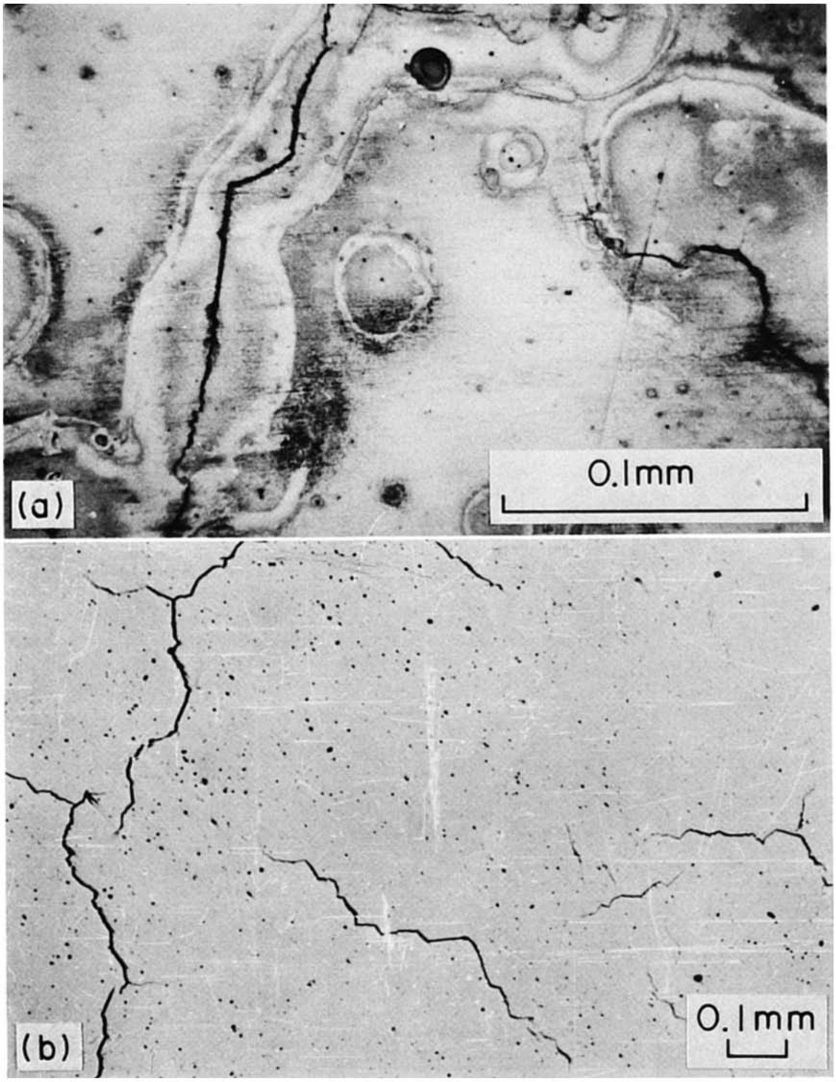

FIG. 12. Stress corrosion cracking of deformed AISI Type 304L stainless steel in de-aerated 0.1M HCl solution at 25°C, 10 min exposure at −600 mV vs SSE (active–passive transition range). Deformation by drawing at liquid nitrogen temperature; deformation degree 30%; transverse surface exposed.
(a) After washing with distilled water, (b) after polishing with 1/4 μm diamond paste.

REFERENCES

1. W. Nicodemi, P. Pedeferri and D. Sinigaglia, *Metallurgia ital.* **63**, 23 (1971).
2. D. Sinigaglia, P. Pedeferri, B. Mazza, G. P. Galliani and L. Lazzari, *Metallurgia ital.* **65**, 77 (1973).
3. B. Mazza, P. Pedeferri, D. Sinigaglia, U. Della Sala and L. Lazzari, *Werkstöffe Korros.* **25**, 239 (1974).
4. A. Cigada and P. Pedeferri, *Annali Chim.* **65**, 509 (1975).
5. B. Mazza, P. Pedeferri, D. Sinigaglia, A. Cigada, L. Lazzari, G. Re and D. Wenger, *J. electrochem. Soc.* **123**, 1157 (1976).
6. A. Cigada, B. Mazza, P. Pedeferri and D. Sinigaglia, *J. Biomed. Mater. Res.* **11**, 503 (1977).
7. A. Cigada, B. Mazza, G. A. Mondora, P. Pedeferri, G. Re and D. Sinigaglia, *Corrosion and Degradation of Implant Materials*, ASTM STP 684, p. 144. ASTM, Philadelphia (1979).
8. G. Re, D. Sinigaglia, D. Wenger and A. Benvenuti, *Metallurgia ital.*, in press.
9. B. Mazza, P. Pedeferri, D. Sinigaglia, A. Cigada, G. A. Mondora, G. Re, G. Taccani and D. Wenger, *J. electrochem. Soc.*, in press.
10. B. E. Wilde and E. Williams, *J. electrochem. Soc.* **117**, 775 (1970).
11. B. E. Wilde and E. Williams, *J. electrochem. Soc.* **118**, 1057 (1971).
12. B. E. Wilde and E. Williams, *Electrochim. Acta* **16**, 1971 (1971).
13. B. E. Wilde, *Corrosion* **28**, 283 (1972).
14. M. Pourbaix, L. Klimzack-Mathieiu, C. Mertens, J. Meunier, A. Van Leugenhaghe, L. de Munck, J. Laureys, L. Neelemans and M. Warzee, *Corros. Sci.* **3**, 239 (1963).
15. E. D. Verink, Jr and M. Pourbaix, *Corrosion* **27**, 495 (1971).
16. B. C. Syrett and S. S. Wing, *Corrosion* **34**, 138 (1978).
17. J. R. Galvele, J. B. Lumsden and R. W. Staehle, *J. electrochem. Soc.* **125**, 1204 (1978).
18. F. Mazza and N. D. Greene, *Proc. 2nd European Symposium on Corrosion Inhibitors*, p. 401. University of Ferrara (1966).
19. G. Bianchi, F. Mazza and S. Torchio, *Proc. 5th International Congress on Metallic Corrosion*, p. 380. NACE, Houston (1974).
20. G. Bianchi, F. Mazza and S. Torchio, *Corros. Sci.* **13**, 165 (1973).